Pergamon

Cement and Concrete Research, Vol. 27, No. 7, pp. 995–1007, 1997

0008-8846/97 $17.00 + .00

PII S0008-8846(97)00102-6

EFFECTS OF CARBONATION ON PORE STRUCTURE AND DIFFUSIONAL PROPERTIES OF HYDRATED CEMENT PASTES

V.T. Ngala and C.L. Page
Aston University, Department of Civil Engineering, Birmingham, UK

(Refereed)
(Received March 26, 1996; in final form May 20, 1997)

ABSTRACT

Steady-state diffusion kinetics of dissolved oxygen and chloride ions were studied in well-cured, partially dried, non-carbonated and fully carbonated specimens of OPC, OPC/30% PFA and OPC/65% BFS pastes. Pore size distribution, total porosity and coarse capillary porosity data for the specimens were also determined. The diffusion resistances of all the materials were adversely affected by pre-drying and carbonation, but the effects were considerably more severe for the blended cements than for the OPC. This was associated with coarsening of the pore structures of the various pastes to differing extents as a result of pre-drying and carbonation. Diffusion rates of both chloride and oxygen in all three carbonated materials appeared to be controlled by a common, purely physical mechanism. © *1997 Elsevier Science Ltd*

Introduction

Diffusion of chloride ions in hydrated cement pastes, mortars and concretes has been studied extensively under steady-state (1-8) and unsteady conditions (9-11). It is well established that the kinetics are affected by several factors, amongst which the nature of the cementitious binder is important. Blended cements containing substantial proportions of fly ash (PFA) or ground granulated blast furnace slag (BFS) sustain far lower rates of chloride diffusion than do Portland cements (OPC) in well-cured specimens of constant water/binder (w/c) ratio (1,2,5,7,8). It is also known, however, that the pore structure and mass transport characteristics of cementitious materials may be strongly influenced by prior exposure to drying and to carbonation (12-14).

Several previous investigations have shown that the resistance to chloride diffusion of hydrated cement systems is adversely affected by carbonation, especially so in the case of blended cements containing PFA or slag (15,16). For many practical situations in which blended cements are used to restrict rates of chloride ingress into concrete structures with a view to extending the corrosion-initiation times of embedded reinforcing steel, eg. in the splash and submerged zones of marine structures (17), it is unlikely that carbonation will affect the properties of the cover concrete to a significant extent because rates of carbonation are very low in predominantly wet environments (18,19). In the cases of structures which are exposed only intermittently to wetting in the presence of chloride salts and to relatively dry

atmospheric conditions for substantial periods, however, it may be expected that the influence of carbonation on the cover concrete will assume greater relevance. In such circumstances, it is also clear that transport mechanisms other than diffusion will affect the rates of ingress of chloride ions.

The aim of the work to be described in this contribution was to provide further evidence and improved understanding of the effects of carbonation on the pore structure and diffusion resistance of a range of well-cured hydrated cement pastes. As in previous studies of non-carbonated systems (7,8), steady-state measurements of the relative diffusion rates of chloride ions and dissolved oxygen molecules were used as a means of assessing the contribution of pore surface-charge effects.

Experimental

Materials and Sample Preparation. The compositions of the OPC, PFA and BFS used, expressed in percentages by weight of the constituent oxides, are shown in Table 1. Blended fly ash and slag cements were obtained from a mixture of OPC with 30%PFA and 65%BFS by weight respectively. The specific surfaces of the OPC and BFS cements were 345 and 410 m^2/kg respectively, while the percentage of PFA retained on a 45 μm sieve was 6.7.

OPC, OPC/30%PFA and OPC/65%BFS pastes were obtained by hand mixing with deionised water for about 5 minutes to produce mixtures of w/c ratios of 0.4, 0.5, 0.6 and 0.7. The mixes were poured into cylindrical PVC containers, 49 mm in diameter by 75 mm in height, and compacted by means of vibration. The cylinders were sealed and rotated end over end at a speed of 8 rpm for at least 24 hours in order to minimise segregation. After curing at 22°C for 2 weeks, the cylinders were demoulded and immersed in 35mM NaOH solution to limit leaching of hydroxyl ions from the paste. They were then stored in a curing room at a temperature of 38 ± 2 °C for 10 weeks in order to accelerate the reactions of fly ash and slag.

Thin discs (approximately 3 mm thick) were cut from the central regions of every cylinder by means of a diamond saw, lubricated with deionized water. Some of the discs were used for mercury intrusion porosimetry (MIP) and diffusion measurements in their non-carbonated state, while the rest were fully carbonated before being used for these experiments. The surfaces of the discs used for diffusion studies were ground with grade 600 emery paper and rinsed with deionised water, before being fitted into the appropriate diffusion cells. For every condition investigated, 4 or 5 replicate cells were set up and placed in a waterbath, which was maintained at a constant temperature of 25°C.

TABLE 1

Chemical Analysis of OPC, PFA and BFS (%)

oxide	CaO	SiO_2	Al_2O_3	Fe_2O_3	SO_3	MgO	Na_2O	K_2O	LOI
OPC	63.58	21.20	5.34	2.62	3.38	1.30	0.09	0.75	1.53
PFA	1.45	48.20	32.20	8.02	0.52	0.66	0.98	2.85	3.84
BFS	40.09	35.51	12.59	0.58	0.15	9.11	0.24	0.54	0.91

Pre-Drying. Some of the cement paste discs were dried from a saturated surface dry condition to constant weight at 65% relative humidity (RH) by storage over saturated solutions of sodium nitrite in desiccators. The air within the desiccators had been pre-treated to remove carbon dioxide. Some of the partially dried discs were further dried as described below and used for MIP, while the rest were resaturated with water and used for chloride diffusion or water desorption measurements.

Carbonation. Carbonation of cement pastes was achieved by exposing the specimens to an atmosphere of 65% relative humidity, containing up to 5% by volume of carbon dioxide. The 65% relative humidity was obtained using a saturated solution of sodium nitrite while the carbon dioxide atmosphere was achieved by passing a gas mixture of 5% CO_2, 95% N_2 for about 30 minutes daily over the specimens in sealed containers. After several weeks, the thickest disc from each set of specimens was tested for carbonation by spraying phenolphthalein pH indicator on the broken surfaces (20). The specimens, when carbonated such that the phenolphthalein was colourless on the broken surfaces, were used for pore structure and diffusion studies.

Oxygen Diffusion. The oxygen diffusion cell used was as described in a previous publication (7). The cell consisted of two compartments containing an anode and a cathode respectively. The cathode compartment was initially filled with a deaerated solution, whilst oxygen gas was bubbled through the anode compartment which also contained a similar solution. 35mM NaOH and deionized water were used as the background solutions for non-carbonated and fully carbonated cement paste specimens respectively. The rate of steady-state diffusion of oxygen was determined electrochemically by the consumption of diffused oxygen repeatedly over a time interval of 2 or 3 days until more than 5 consistent values of the flux were obtained. The effective diffusion coefficients of oxygen (D_O) were calculated from Fick's first law and Faraday's law as described in the previous paper (7).

Chloride Diffusion. Chloride diffusion experiments were carried out in parallel to oxygen diffusion experiments for a set of accompanying specimens. This was achieved by use of the ionic diffusion cell described elsewhere (2). At the start of the experiment for non-carbonated specimens, the high concentration side of the cell was filled with a solution containing 1M NaCl in 35mM NaOH while the low concentration side was filled with 35mM NaOH solution. On the other hand, 1M NaCl and deionized water were used as the starting solutions during experiments on carbonated cement pastes. The quantities of chloride diffusing to the low concentration side were determined by means of a standard spectrophotometric technique (21). The calculation of the effective diffusion coefficient of chloride (D_{Cl}) was described in a previous publication (2).

Pore Structure. Pore size distribution studies by MIP were performed on replicates of the specimens used for diffusion measurements. In order to minimize the influence of drying on pore structure, the water in the specimens was removed by iso-propanol treatment followed by evacuation, as recommended by previous researchers (22,23).

After the oxygen diffusion experiments, the water-saturated discs were removed from their cells and used for bulk density and porosity measurements. The specimens were dried at 90.7% relative humidity by placing them above a saturated salt solution of barium chloride contained in a desiccator and the weight recorded at intervals until the change in weight was negligible. The weight loss on drying was then converted to volume fraction of the bulk

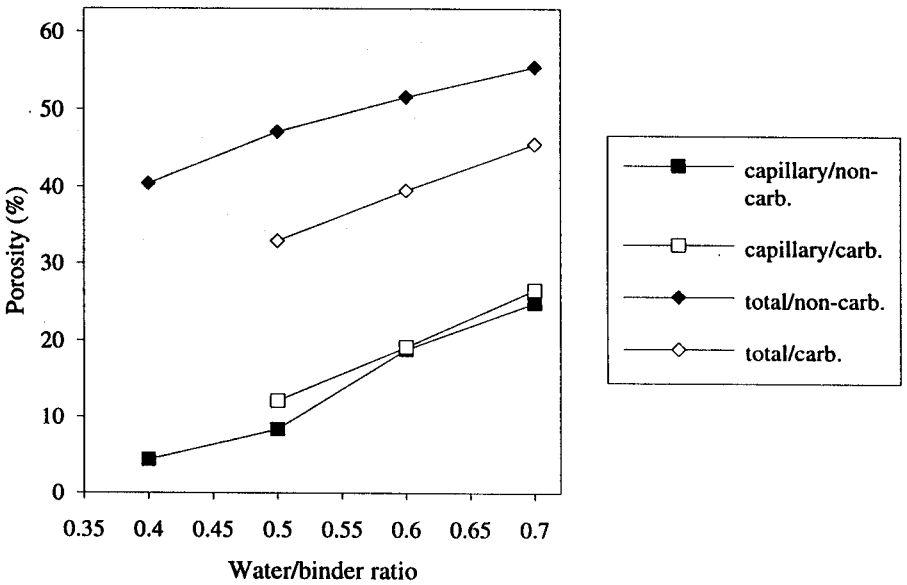

FIG. 1.
Porosity of non-carbonated and carbonated OPC pastes.

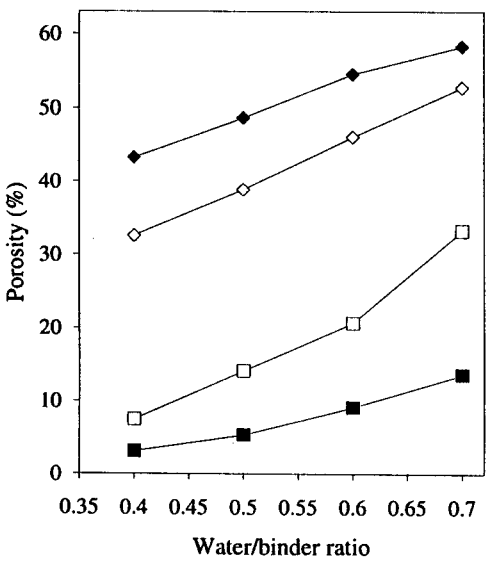

FIG. 2.
Porosity of non-carbonated and carbonated fly ash pastes (Key as for Fig. 1).

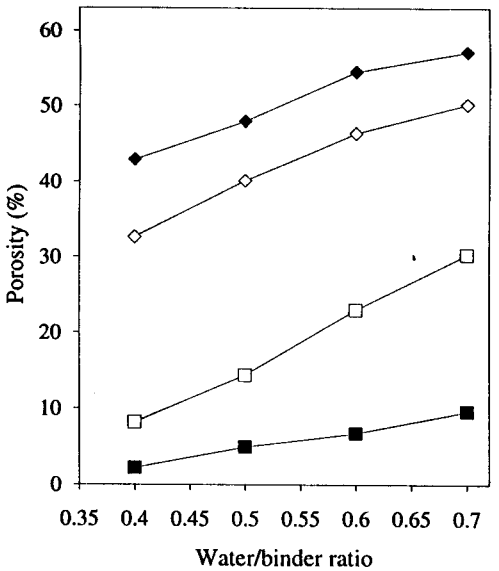

FIG. 3.
Porosity of non-carbonated and carbonated slag pastes (Key as for Fig. 1).

paste. This particular measure of coarse capillary porosity corresponds to pores wider than about 30 nm (24) and was used because:

(i) it avoided unrealistic drying, which can produce porosity artefacts (25),
(ii) it was found to correlate with another transport property, rate of water absorption (24).

The specimens were finally dried at 105°C and the total porosity values calculated.

Results and Discussion

The experimentally obtained effective diffusion coefficients, total porosities and the volume fractions of the water lost on drying at 90.7% relative humidity showed very close consistency between the replicate samples. Full details of these results have been presented elsewhere (26).

Pore Structure. The alteration in the porosity of hardened cement pastes as a result of carbonation is shown in Figures 1, 2 and 3 for OPC, OPC/30% PFA and OPC/65%BFS pastes respectively. These figures indicate that there was a reduction in the total porosity of the three cement systems with carbonation, but a redistribution of the pore sizes; the proportion of large capillary pores (diameter > 30 nm) was increased slightly for the OPC pastes but much more significantly so for the fly ash and slag pastes. There was no significant increase in the capillary porosity of OPC pastes following carbonation, as reported in the literature (14). However, the average increases for OPC/30%PFA and OPC/65% BFS pastes were 140% and 230% respectively.

The pore structure of carbonated cement pastes was also investigated by MIP, the results being broadly compatible with the porosity changes described above. The total porosity and total intrusion volume obtained from desorption and MIP techniques respectively are shown

TABLE 2

Total Pore Volumes of Hardened Cement Pastes

Binder	W/C Ratio	Total Porosity (cm^3/g)		Total Intrusion Volume (cm^3/g)	
		Non-carbonated	Carbonated	Non-carbonated	Carbonated
OPC	0.4	0.404	-	0.098	-
	0.5	0.475	0.329	0.161	0.093
	0.6	0.529	0.395	0.225	0.144
	0.7	0.554	0.455	0.264	0.201
OPC/30%PFA	0.4	0.433	0.326	0.139	0.064
	0.5	0.487	0.389	0.194	0.150
	0.6	0.553	0.462	0.248	0.184
	0.7	0.583	0.528	0.262	0.290
OPC/65%BFS	0.4	0.430	0.326	0.143	0.093
	0.5	0.480	0.402	0.206	0.169
	0.6	0.545	0.465	0.278	0.204
	0.7	0.572	0.503	0.290	0.228

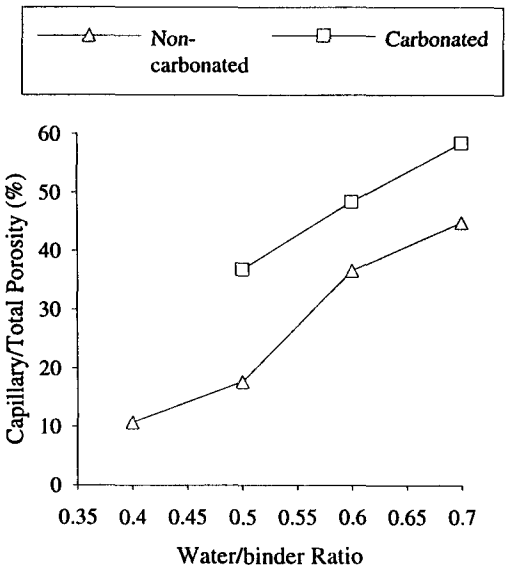

FIG. 4.
Ratio of capillary to total porosity for OPC pastes from water desorption measurements.

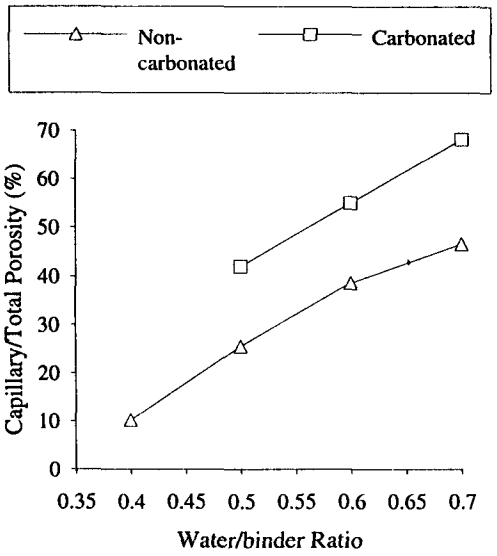

FIG. 5.
Ratio of capillary to total porosity for OPC pastes from MIP measurements.

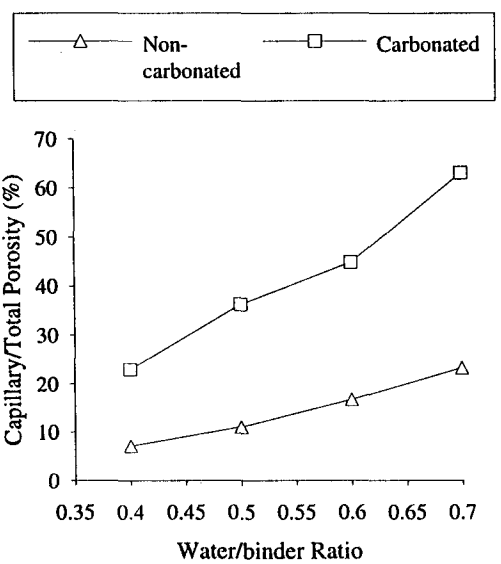

FIG. 6.
Ratio of capillary to total porosity for PFA pastes from water desorption measurements.

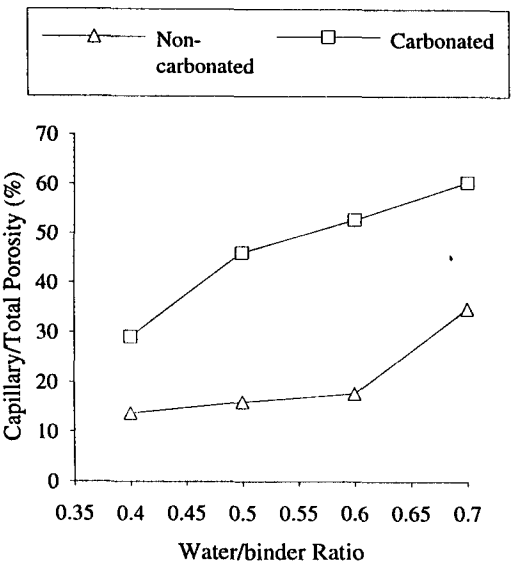

FIG. 7.
Ratio of capillary to total porosity for PFA pastes from MIP measurements.

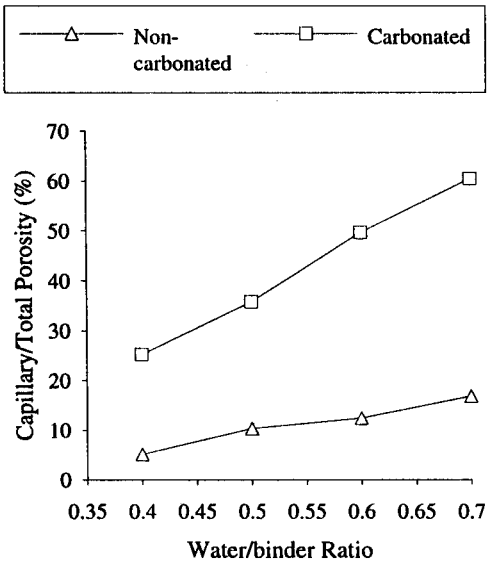

FIG. 8.
Ratio of capillary to total porosity for BFS pastes from water desorption measurements.

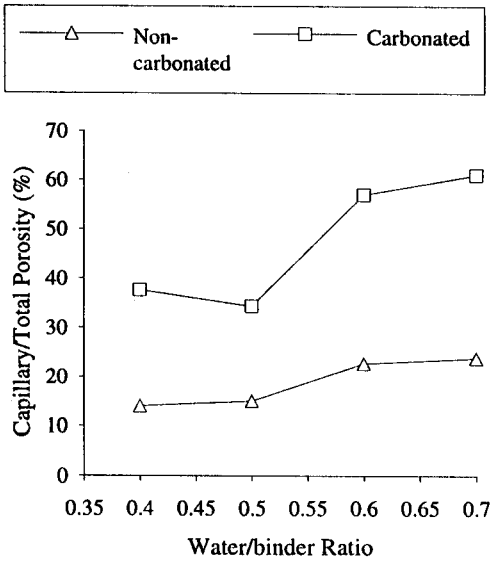

FIG. 9.
Ratio of capillary to total porosity for BFS pastes from MIP measurements.

in Table 2. The corresponding bulk densities of the cement pastes shown in Table 2 have been presented elsewhere (26). The ratio of the coarse capillary pore volume to the total pore volume has been adopted in this study to compare the measurements from the two techniques, as shown in Figures 4 to 9. These figures demonstrate essentially similar trends from both desorption and MIP techniques for OPC, OPC/30% PFA and OPC/65% BFS pastes. It is recognised, however, that MIP tends to provide distorted measurements of the size-distribution of the coarsest pores (~1μm) because intrusion pressures depend on the neck dimensions rather than the bulk dimensions of the pores (27).

The reduction in total pore volume observed for the three cement matrices could be associated with the deposition of the $CaCO_3$ formed during carbonation. The volume of the $CaCO_3$ formed exceeds that of the hydrates from which it is formed, thus causing a reduction in total porosity. On the other hand, the coarsening of the pore structure may be associated with the formation of additional silica gel due to the decomposition of the C-S-H gel in the matrices following prolonged exposure to CO_2 (14). Furthermore, the variation in the degree of alteration of the pore structure for the various binders indicates the differences in their original compositions and amount of cement hydrates prior to carbonation. The pozzolanic reaction of PFA and the hydraulicity of slag in blended cement pastes reduce the amount of $Ca(OH)_2$ crystals, producing additional C-S-H gel which can be decomposed to form silica gel (14).

A redistribution of pore sizes was also observed in specimens partially dried to 65% relative humidity, though on a smaller scale compared to the effect of carbonation as shown in Table 3. In this case, both techniques revealed a significant increase in the proportion of large capillary pores in all three cement systems, with no noticeable change in the total pore volume.

TABLE 3

Porosity of Saturated and Pre-Dried Hardened Cement Pastes.

Binder	W/C Ratio	Porosity of Saturated Pastes (cm^3/g)		Porosity of Pre-Dried Pastes (cm^3/g)	
		Capillary	Total	Capillary	Total
OPC	0.5	0.084	0.475	0.134	0.481
	0.6	0.188	0.529	0.200	0.533
OPC/30%PFA	0.5	0.053	0.487	0.065	0.499
	0.6	0.091	0.553	0.101	0.561
OPC/65%BFS	0.5	0.050	0.480	0.062	0.497
	0.6	0.068	0.545	0.105	0.550

Diffusional Properties. Effective chloride diffusion coefficients are shown, in Figure 10, to increase markedly as the capillary porosity increases for non-carbonated OPC pastes. For non-carbonated OPC/30% PFA and OPC/65% BFS pastes, the corresponding changes in D_{Cl} are much more gradual, as shown in Figures 11 and 12. The figures also illustrate the effect of partial drying on the effective chloride diffusion coefficients in the three cement matrices. It may be seen that the influence of drying is more marked in the blended cement pastes, than in OPC specimens, with OPC/65% BFS pastes sustaining the greatest impairment of their resistance to chloride diffusion.

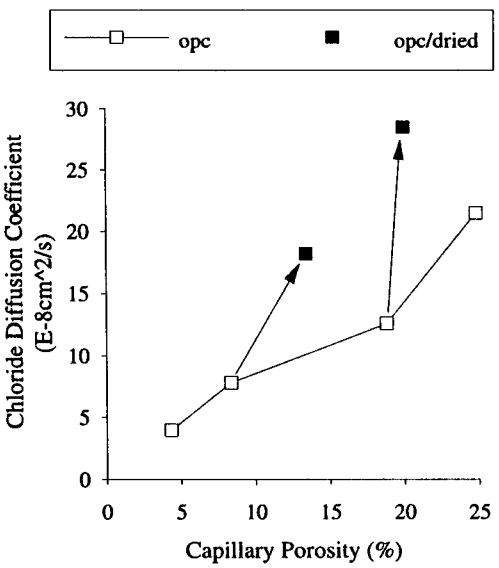

FIG. 10.
Chloride diffusivity against capillary porosity for non-carbonated OPC pastes.

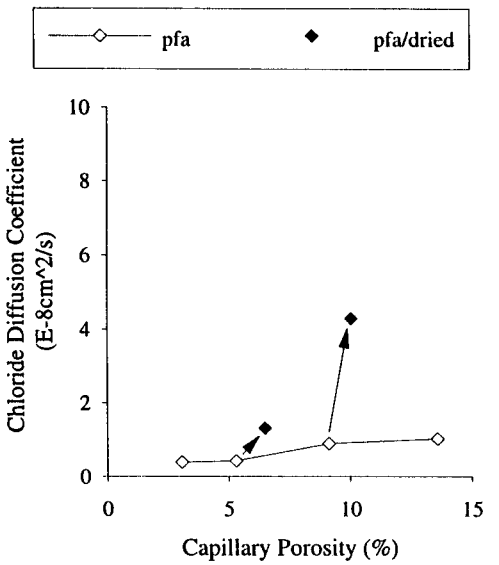

FIG. 11.
Chloride diffusivity against capillary porosity for non-carbonated PFA pastes.

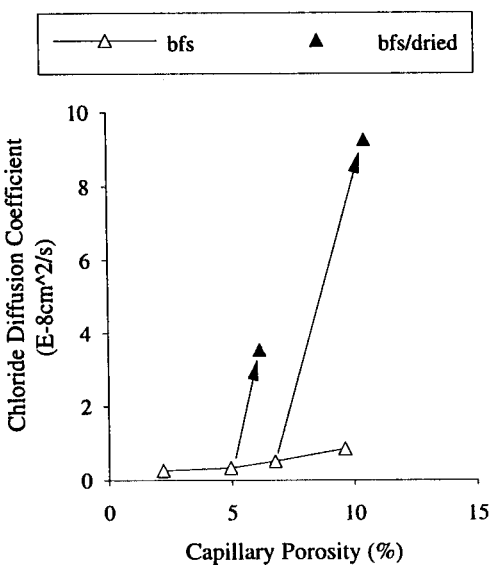

FIG. 12.
Chloride diffusivity against capillary porosity for non-carbonated BFS pastes.

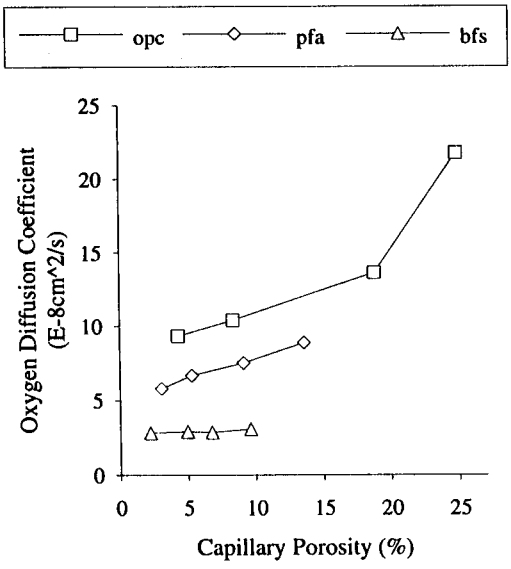

FIG. 13.
Oxygen diffusivity against capillary porosity for non-carbonated cement pastes.

Figure 13 demonstrates that the effective diffusion coefficients of oxygen increase as the capillary porosity increases for the OPC and OPC/30% PFA pastes, but that the effect is insignificant for the OPC/65% BFS pastes. It is also evident from these figures that for the same coarse capillary porosity, oxygen molecules diffuse at different rates in the OPC,

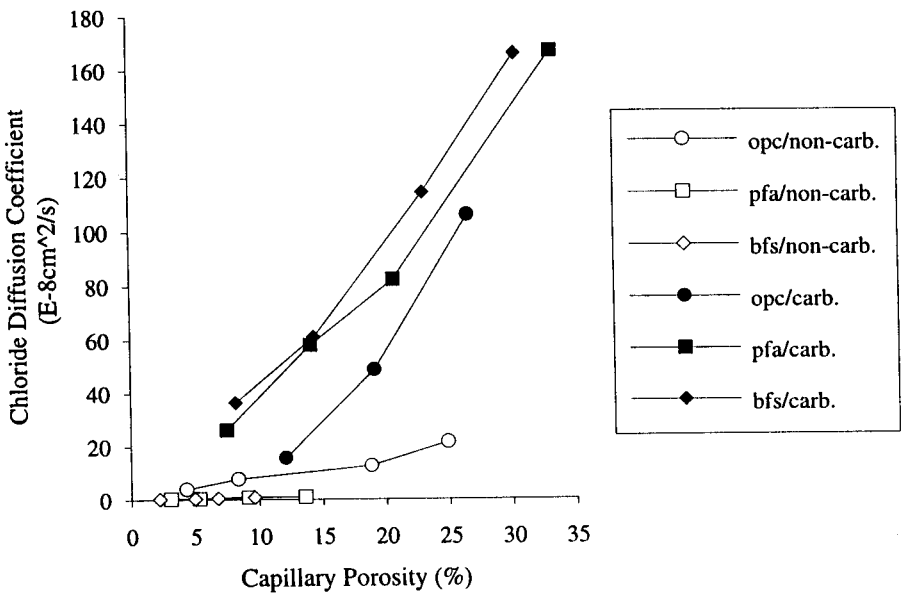

FIG. 14.
Chloride diffusion coefficients for carbonated and non-carbonated cement pastes.

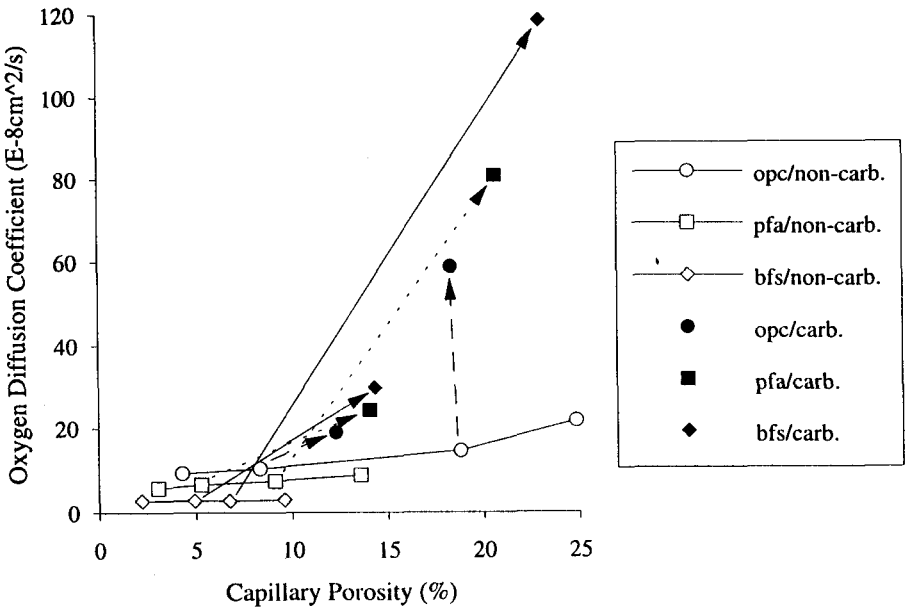

FIG. 15.
Oxygen diffusion coefficients for carbonated and non-carbonated cement pastes.

OPC/30%PFA and OPC/65%BFS pastes. These differences in oxygen diffusion rates are liable to be associated with physical differences in the connectivity or tortuosity of the pore systems within the non-carbonated cement pastes.

Carbonation of cement pastes has a large effect on their diffusional properties, more so for the blended pastes than for plain OPC pastes. The rate of chloride diffusion in blended

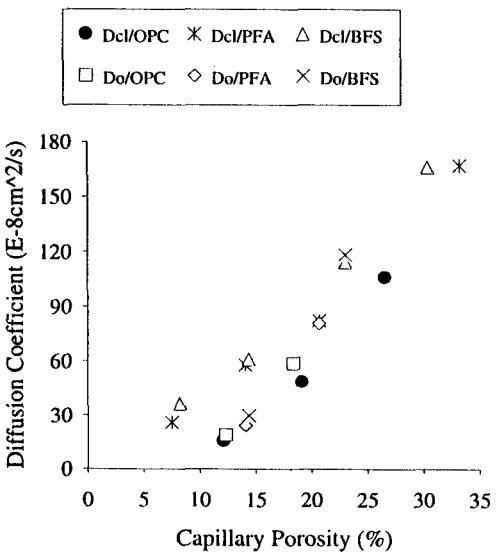

FIG. 16.
Chloride and oxygen diffusivities versus capillary porosity for carbonated pastes.

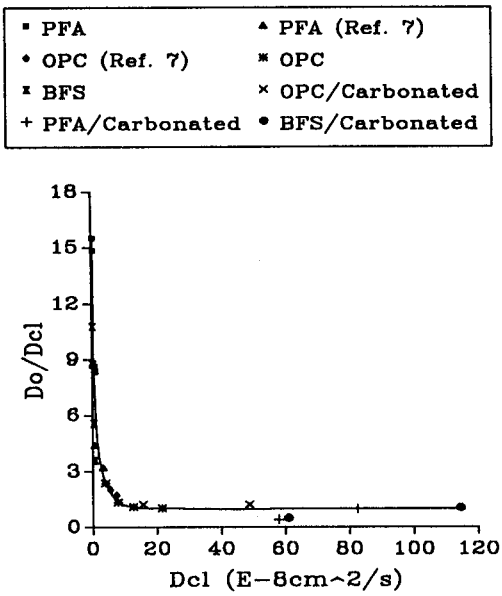

FIG. 17.
Ratio of oxygen to chloride diffusion coefficient for hydrated cement pastes.

pastes following carbonation increases by two orders of magnitude (Figure 14) while oxygen diffusion rates increase by one order of magnitude (Figure 15). Figure 16 shows that for fully carbonated pastes, the relationship between effective chloride diffusion coefficient and capillary porosity is very similar to that between effective oxygen diffusion coefficient and capillary porosity. Furthermore, this figure demonstrates that the relationship is roughly constant, irrespective of the cement binder used.

The ratio of oxygen to chloride diffusion coefficients (D_O/D_{Cl}) was considered in previous studies (7,8) to provide a measure of the effect of pore surface charge on chloride diffusion for non-carbonated cement pastes. The results obtained for fully carbonated pastes are illustrated in Figure 17, together with the previous data (7,8). This figure shows that the ratio tends to 1 for coarse-textured carbonated pastes (and OPC pastes of high w/c ratio) but can attain high values (>10) for fine-textured blended cement pastes which have not suffered drying/carbonation. This confirms previous conclusions (7,8) regarding the effects of pore geometry and surface charge on chloride ion transport. Thus the results in Figures 16 and 17 suggest that, in fully carbonated, water-saturated OPC, OPC/30% PFA and OPC/65% BFS pastes, the rates of diffusion of chloride ions and oxygen molecules are controlled by a common, purely physical mechanism. This is in contrast to the rate-controlling processes for chloride diffusion in non-carbonated, hydrated cement pastes, which are believed to depend on ion-pore surface interactions (2,3,7,8).

Conclusions

The pore structure of hardened cement pastes is altered by exposure to drying or carbonation, the extent of the alteration depending on the type of binder used. There is a reduction in

total porosity for OPC, OPC/30%PFA and OPC/65%BFS pastes as a result of carbonation but a redistribution of pore sizes; the proportion of large pores (diameter > 30 nm) is increased slightly for OPC pastes but much more significantly so for the fly ash and slag pastes. Similar trends are discernable from porosity data obtained by water desorption and MIP.

Pre-drying of specimens to 65% RH causes a substantial increase in their effective chloride diffusion coefficients and this effect is particularly noticeable for blended cement binders, whose resistance to chloride diffusion prior to drying exhibits less sensitivity to increase in w/s ratio (coarse capillary porosity) than that of OPC.

Carbonation has a much larger effect than does drying on chloride diffusion resistances (and oxygen diffusion resistances) of hardened cement pastes. For non-carbonated specimens, every binder exhibits an individual relationship between diffusion coefficient and coarse capillary porosity; for carbonated specimens, there is a roughly constant relationship between diffusion coefficient and coarse capillary porosity. This applies for oxygen as well as chloride.

The ratio of oxygen to chloride diffusion coefficients (D_O/D_{Cl}) tends to 1 for coarse-textured carbonated pastes (and OPC pastes of high w/c ratio) but can attain high values (>10) for fine-textured blended cement pastes which have not suffered drying/carbonation. This confirms previous conclusions regarding the effects of pore geometry and surface charge on chloride ion diffusion.

From a practical viewpoint, it should be noted that blended cement concretes, incorporating PFA or BFS, may be expected to exhibit high resistance to chloride diffusion in the cover zone to reinforcement if they are well-cured and exposed to permanently wet service environments where carbonation is unlikely to be significant, e.g. in the splash and submerged zones of marine structures. This may not apply, however, to situations where concrete structures are exposed to prolonged drying and carbonation.

Acknowledgements

The authors thank the Overseas Research Students (ORS) Awards Scheme and the James Watt Fellowship, who through their sponsorship and support, made this study possible. They also thank Dr L.J. Parrott for stimulating discussions.

References

1. H. Ushiyama and S. Goto, Proc. 6th Int. Congr. Chem. Cement, Moscow, Vol. II-1, 331 (1974).
2. C.L. Page, N.R. Short and A. El Tarras, Cem. Concr. Res., 11, 395 (1981).
3. S. Goto and D.M. Roy, Cem. Concr. Res., 11, 751 (1981).
4. A. Atkinson and A.K. Nickerson, J. Mater. Sci., 19, 3036 (1984).
5. P. Lambert, C.L. Page and N.R. Short, British Ceramics Proc., No.35, 267 (1984).
6. H. Uchikawa, S. Uchida and K. Ogawa, Review of the 38th General Meeting of Cement Association of Japan, 14, 56 (1984).
7. S.W. Yu and C.L. Page, Cem. Concr. Res., 21, 581 (1991).
8. V.T. Ngala, C.L. Page, L.J. Parrott and S.Y. Yu, Cem. Concr. Res., 25, 819 (1995).
9. M. Collepardi, A. Marcialis and R. Turriziani, Il Cemento, 69, 143 (1972).
10. G. Sergi, S.W. Yu and C.L. Page, Mag. Concr. Res., 44, 63 (1992).
11. S.W. Yu, G. Sergi and C.L. Page, Mag. Concr. Res., 45, 257 (1993).

12. H.K. Hilsdorf, J. Kropp and M. Gunter, Proc. RILEM Seminar, Hanover, p. 182 (1984).
13. R.G. Patel, L.J. Parrott, J.A. Martin and D.C. Killoh, Cem. Concr. Res., 15, 343 (1985).
14. T.A. Bier, Mater. Res. Soc. Symp. Proc., Boston, 85, 18 pp. (1986).
15. R.K. Dhir, M.R. Jones and M.J. McCarthy, Proc. Instn. Civ. Engrs: Structs and Bldgs, 99, 167 (1993).
16. H.-J. Wierig and H. Langkamp, ZKG International, 48, 184 (1995).
17. P.B. Bamforth and W.F. Price, Concrete 2000-Economic and Durable Construction through Excellence, Dundee, 7-9 Sept., p. 1105 (1993).
18. G.J. Osborne, Proc. 3rd Int. Conf. on Fly Ash, Silica Fume, Slag and Natural Pozzolans in Concrete, SP 114-59, Trondheim, Norway, p. 1209 (1989).
19. L.J. Parrott, A Review of Carbonation in Reinforced Concrete, BRE/C&CA Report C/1-987, 126pp. (1987).
20. J. Forrester, Carbonation of Concrete, RILEM Symp., paper 2.1, 6 pp. (1976).
21. I.A. Vogel, A Textbook of Quantitative Inorganic Analysis, 4th ed., p. 754 (1978).
22. R. Feldman and J.J. Beaudoin, Cem. Concr. Res., 21, 297 (1991).
23. L. Konecny and S.J. Naqvi, Cem. Concr. Res., 23, 1223 (1993).
24. L.J. Parrott, Cem. Concr. Res., 22, 1077 (1992).
25. L.J. Parrott, Mater. Res. Symp. Proc., 85, 91 (1987).
26. V.T. Ngala, PhD Thesis, Aston University, Birmingham, UK (1995).
27. S. Diamond and M.E. Leeman, Mat. Res. Soc. Symp. Proc., Boston, 370, 217 (1995).